Research Article | Vol. 25, No. 2 | 23 Jan 2017 | OPTICS EXPRESS 874

Optics EXPRESS

Electro-tunable liquid crystal laser based on high-Q Fabry-Pérot microcavity

WONSUK LEE,[1] WENJIE WANG,[2] GUKSIK LEE,[1] SEONG HO RYU,[1] XUDONG FAN,[2,3,4] AND DONG KI YOON[1,5]

[1]*Graduate School of Nanoscience and Technology and KINC, Korea Advanced Institute for Science and Technology, Daejeon, 34141, South Korea*
[2]*Key Lab of Advanced Transducers and Intelligent Control System of Ministry of Education, Taiyuan University of Technology, 79 Yingze Street, Taiyuan 030024, China*
[3]*Department of Biomedical Engineering, University of Michigan, Ann Arbor, 1101 Beal Ave., Ann Arbor, Michigan 48109, USA*
[4]*xsfan@umich.edu*
[5]*nandk@kaist.ac.kr*

Abstract: We demonstrate an electro-tunable laser based on a plano-concave (p-c) Fabry-Pérot (FP) microcavity filled with dye-doped liquid crystal (LC) gain material. Owing to the high Q-factor of the p-c FP microcavity, the lasing threshold of the LC laser is as low as 0.58 μJ/mm^2. The single-mode emission wavelength can be easily tuned by varying applied voltage, which induces the reconfiguration of LC molecules. Furthermore, this lasing platform operates at room temperature, thanks to the wide temperature range of the nematic LC. We believe that our LC laser is widely applicable to light sources of various micro total analysis systems.

© 2016 Optical Society of America

OCIS codes: (140.0140) Lasers and laser optics; (140.2050) Dye lasers; (140.3948) Microcavity devices; (160.3710) Liquid crystals; (230.3720) Liquid-crystal devices.

References and links

1. C. V. Shank, "Physics of dye lasers," Rev. Mod. Phys. **47**(3), 649–657 (1975).
2. A. E. Siegman, *Lasers* (University Science Books, 1986).
3. X. Fan and S. H. Yun, "The potential of optofluidic biolasers," Nat. Methods **11**(2), 141–147 (2014).
4. Y. Sun, S. I. Shopova, C. S. Wu, S. Arnold, and X. Fan, "Bioinspired optofluidic FRET lasers via DNA scaffolds," Proc. Natl. Acad. Sci. U.S.A. **107**(37), 16039–16042 (2010).
5. W. Lee and X. Fan, "Intracavity DNA melting analysis with optofluidic lasers," Anal. Chem. **84**(21), 9558–9563 (2012).
6. Y. Sun and X. Fan, "Distinguishing DNA by analog-to-digital-like conversion by using optofluidic lasers," Angew. Chem. Int. Ed. Engl. **51**(5), 1236–1239 (2012).
7. D. Psaltis, S. R. Quake, and C. Yang, "Developing optofluidic technology through the fusion of microfluidics and optics," Nature **442**(7101), 381–386 (2006).
8. C. Monat, P. Domachuk, and B. J. Eggleton, "Integrated optofluidics: A new river of light," Nat. Photonics **1**(2), 106–114 (2007).
9. Z. Li and D. Psaltis, "Optofluidic dye lasers," Microfluid. Nanofluidics **4**(1-2), 145–158 (2008).
10. W. Lee, H. Li, J. D. Suter, K. Reddy, Y. Sun, and X. Fan, "Tunable single mode lasing from an on-chip optofluidic ring resonator laser," Appl. Phys. Lett. **98**(6), 061103 (2011).
11. T. Uchida, "40 years research and development on liquid crystal displays," Jpn. J. Appl. Phys. **53**(3S1), 03CA02 (2014).
12. H. Coles and S. Morris, "Liquid-crystal lasers," Nat. Photonics **4**(10), 676–685 (2010).
13. M. Ozaki, M. Kasano, T. Kitasho, D. Ganzke, W. Haase, and K. Yoshino, "Electro-Tunable Liquid-Crystal Laser," Adv. Mater. **15**(12), 974–977 (2003).
14. T.-H. Lin, Y.-J. Chen, C.-H. Wu, A. Y. G. Fuh, J. H. Liu, and P. C. Yang, "Cholesteric liquid crystal laser with wide tuning capability," Appl. Phys. Lett. **86**(16), 161120 (2005).
15. S. M. Morris, P. J. W. Hands, S. Findeisen-Tandel, R. H. Cole, T. D. Wilkinson, and H. J. Coles, "Polychromatic liquid crystal laser arrays towards display applications," Opt. Express **16**(23), 18827–18837 (2008).
16. M. Y. Jeong and K. Kwak, "Active thermal fine laser tuning in a broad spectral range and optical properties of cholesteric liquid crystal," Appl. Opt. **55**(33), 9378–9383 (2016).
17. M. Y. Jeong and J. W. Wu, "Continuous spatial tuning of laser emissions in a full visible spectral range," Int. J. Mol. Sci. **12**(3), 2007–2018 (2011).

#280215 http://dx.doi.org/10.1364/OE.25.000874
Journal © 2017 Received 4 Nov 2016; revised 6 Jan 2017; accepted 6 Jan 2017; published 11 Jan 2017

Optics EXPRESS

18. M. Y. Jeong and J. Cha, "Firsthand in situ observation of active fine laser tuning by combining a temperature gradient and a CLC wedge cell structure," Opt. Express **23**(16), 21243–21253 (2015).
19. W. Wang, C. Zhou, T. Zhang, J. Chen, S. Liu, and X. Fan, "Optofluidic laser array based on stable high-Q Fabry-Pérot microcavities," Lab Chip **15**(19), 3862–3869 (2015).
20. J. Li, S. Gauza, and S.-T. Wu, "Temperature effect on liquid crystal refractive indices," J. Appl. Phys. **96**(1), 19–24 (2004).
21. D. Hunger, C. Deutsch, R. J. Barbour, R. J. Warburton, and J. Reichel, "Laser micro-fabrication of concave, low-roughness features in silica," AIP Adv. **2**(1), 012119 (2012).
22. D. Porter, J. R. Savage, I. Cohen, P. Spicer, and M. Caggioni, "Temperature dependence of droplet breakup in 8CB and 5CB liquid crystals," Phys. Rev. E Stat. Nonlin. Soft Matter Phys. **85**(4), 041701 (2012).
23. J. Li, C. H. Wen, S. Gauza, R. Lu, and S. T. Wu, "Refractive Indices of Liquid Crystals for Display Applications," J. Disp. Technol. **1**(1), 51–61 (2005).
24. W. Cao, P. Palffy-Muhoray, B. Taheri, A. Marino, and G. Abbate, "Lasing Thresholds of Cholesteric Liquid Crystals Lasers," Mol. Cryst. Liq. Cryst. (Phila. Pa.) **429**(1), 101–110 (2006).

1. Introduction

Laser light source is tremendously useful in optical detection/analysis systems, owing to its coherence, controlled polarization, and monochromaticity [1–3]. A laser device with tunable wavelength would be particularly attractive as the light source in a micro total analysis system (μTAS), also known as a lab-on-a-chip, for biochemical sensing, since various dyes are utilized to stain the biomolecular analyte in the optical sensing platforms [3–6]. Optofluidic lasers [7–9] have been intensively investigated for these applications, due to their superior lasing characteristics and long-range wavelength tunability that is obtained by exchanging the liquid gain medium in the fluidic channel. However, despite a change in refractive index of the gain medium can result in a fine-tuning of the laser wavelength [10], a rapid, continuous, and fine tuning is difficult to realize, since the refractive index of an isotropic medium cannot be easily modified.

Over 50 years, liquid crystals (LCs) have been introduced in optical devices because of their high birefringence and molecular reconfigurability, enabling to realize LC display (LCD), which is nowadays a well-established technology with unprecedented performance and reliability [11]. While the majority of LCD devices utilize LCs exhibiting a nematic phase, which is the least ordered mesophase, higher-ordered LC phases that allow photonic bandgap formation possess great potential for laser devices [12]. A number of researchers have recently created band-edge LC lasers with cholesteric-, smectic-, and cholesteric blue-phase LCs, all of which are capable of continuously tuning the laser wavelength by varying temperature, electric field or wedge structures [12–17]. However, these band-edge LC lasers have lasing thresholds much higher than the optofluidic lasers mentioned above, because of the limited light confinement of the naturally formed photonic structures, and thus need further studies to be applicable to light sources of the miniaturized systems. The photonic structures, for example, the chiral pitch of the cholesteric LC (CLC) material, vary by temperature change, which allows the output laser wavelength tuning; however, at the same time, this requires precise control over operating temperature of the band-edge LC lasers in order to obtain the desired laser wavelength. Even worse, since the highly ordered LC phases, such as smectic and blue-phase, intrinsically show very narrow temperature ranges [12]. Control of temperature is complicated compared to applying voltage / electric-field in the miniaturized system, which critically limits applications of LC lasers in μTAS.

In this work, we propose and demonstrate an LC laser device with the simplest form of laser cavity filled with a dye-doped nematic LC material gain. The proposed laser device is based on a recently realized Fabry-Pérot (FP) microcavity [18] that has plano-concave (p-c) structure with a high Q-factor, which is orders of magnitude higher than that of a conventional plano-plano (p-p) FP microcavity. Because of the high Q-factor as well as a bulk interaction between the mode-confined light and the dye-doped LC gain, the lasing threshold of the proposed LC laser is as low as 0.58 μJ/mm^2. The LC-filled p-c FP microcavity resembles a typical LCD device with a simple vertical alignment (VA) sandwich cell configuration, in which the change in the long-range ordering of the LC molecules results

Optics EXPRESS

in the laser emission wavelength tuning rather than an on/off behavior of the VA-LCD. A single-mode laser emission with narrow bandwidth is easily obtained by a small sandwich cell gap (~5 μm), which corresponds to the sufficiently large free spectral range (FSR) of the laser cavity, and the emission wavelength can be continuously tuned by applying voltage to the LC sandwich cell. The nematic LC material is adaptable to any dispersible guest dye molecules. Therefore, a long-range wavelength tuning is also possible by simply exchanging dyes without any modification on the host LC material and photonic structure. Moreover, our laser can be operated at room temperature and has a reliable performance against temperature variations because a commercially available nematic-phase LC material is utilized [19], which is well engineered to cover wide temperature range.

2. Experimental

The preparation of the p-c FP microcavity is based on a microwell fabrication technique [18]. The microwell is produced on the optically polished surface of a fused silica glass substrate by the CO_2 laser ablation method [20], which is a simple process that can provide smooth microwell surface. An RF-pumped CO_2 laser (Synrad's firestar vi30, pulse repetition rate = 20 kHz) is focused by a ZnSe lens with a focal length of 25.4 mm and incident normally to the substrate. As characterized previously [18], a CO_2 laser power of ~0.9 W and 30 ms pulse duration time, results in a microwell with ~3 μm in depth, ~40 μm in diameter, and ~200 μm in curvature radius. An array of microwells with a period of 3 mm is successfully fabricated on the 2 cm × 2 cm × 1 mm glass substrate.

The two glass substrates with and without the microwell array are coated with distributed Bragg reflection (DBR) dielectric layers. The DBR coating consists of 15 pairs of SiO_2 and Ta_2O_5 layers, and has a reflectivity at the center wavelength of 650 nm higher than 99.9%. An indium tin oxide (ITO) layer of 150 nm thickness is subsequently sputtered on these DBR-coated substrates to serve as transparent electrodes and provide a planar anchoring to the LC medium, at the same time. Then, the two glass substrates are assembled to make a sandwich cell with a fixed cell gap using 5 μm silica beads. A 1 wt% 4-(dicyanomethylene)-2-methyl-6-(4-dimethylaminostyryl)-4H-pyran (DCM) laser dye is dispersed in 4-cyano-4'-pentylbiphenyl (5CB) LC molecule, and this dye-doped LC material is subsequently infiltrated to the sandwich cell by a capillary action. Even though a larger portion of the laser dye improves lasing characteristics such as lower lasing threshold, the dye content is limited to 1 wt%, because an excessive amount of dye molecules may disturb the alignment of the LC molecules.

Figures 1(a) and 1(b) show the schematics of the operating LC laser. The p-c FP microcavity has stable light confinement against any misalignment of the two substrates [18], and thus the high Q-factor can be maintained during cavity assembly. The lasing signal emerges from both the top and bottom sides of the sandwich cell. Since the 5CB molecule has the nematic LC phase in the temperature range from 18 °C to 35 °C [21], the dye-doped LC gain medium shows the nematic phase at room temperature. When there is no applied voltage, the LC molecules are aligned parallel to the substrates due to the planar anchoring of the ITO layer, in which typical Schlieren textures are observed by a polarized optical microscopy (POM) as shown in Fig. 1(c). On the other hand, since 5CB has a positive dielectric constant, an electric field (voltage) applied to the sample re-aligns the LC molecules perpendicular to the substrates, and thus a dark state is observed as depicted in Fig. 1(d).

The LC laser with the sandwich cell filled with the dye-doped LC gain is pumped with an optical parametric oscillator (OPO) (Continuum, 5 ns pulsed laser, 20 Hz repetition rate) with 470 nm wavelength. The pump laser is incident normally to the cell and focused on the single microwell through a confocal setup, and the resulting laser emission is simultaneously collected by a spectrometer (HR550i, Horiba Jobin Yvon).

Optics EXPRESS

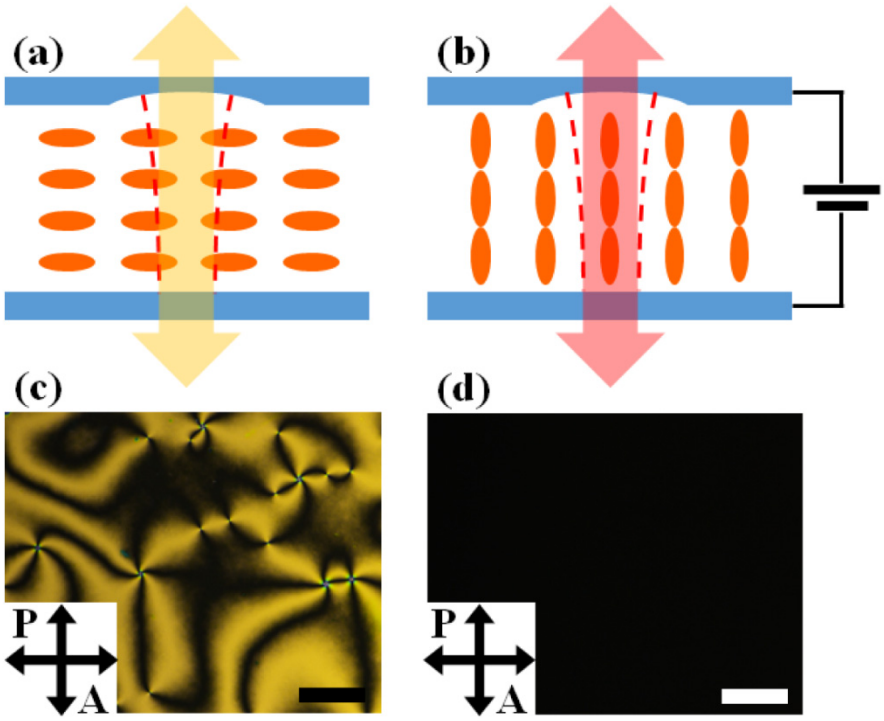

Fig. 1. Schematics of the LC laser with p-c FP microcavity during operation. (a) Horizontally-aligned dye-doped LC molecules interact with light confined in the microcavity providing an optical feedback for lasing. The laser signal emerges from both the top and bottom sides of the sandwich cell. (b) When the electric field is applied to the top and bottom electrodes of the sandwich cell, the LC molecules are vertically aligned, in which the confined light passing through the sample experiences a different refractive index, owing to the birefringence of the LC molecules. POM images of the sandwich cell (c) without / (d) with applied electric field, showing typical planar and homeotropic aligned nematic LC textures, respectively. Since the normally incident light with perpendicular polarization does not experience any birefringence, the backlight is blocked by the analyzer, presenting the dark state in (d). Scale bar = 100 μm.

3. Results and discussion

Figure 2 presents representative output emission spectra of the LC laser (a) and spectrally integrated laser-emission intensity as a function of the pump energy density (b). The single p-c FP microcavity is optically pumped with the OPO at a pump energy-density of 3.2 μJ/mm^2, and the corresponding laser emission depicted by the red curve in Fig. 2(a) shows a single-mode lasing spectrum with a narrow bandwidth, indicating our LC laser has the high Q-factor. All the LC molecules are horizontally aligned without any long-range ordering as observed in Fig. 1(c). Laser light confined in the microcavity has the polarization perpendicular to the propagating direction, thus in the same plane with LC molecules, and experiences azimuthally random distributed LC molecules. Consequently, an effective refractive index is an average of the ordinary refractive index, n_o, and the extraordinary refractive index, n_e, of 5CB LC, which is approximately 1.61 for 650 nm wavelength light [22]. The corresponding FSR of the FP cavity is calculated to be 16.5 nm, considering the cell gap of the sandwich cell and the depth of the microwell (total microcavity length of 8 μm), and it is large enough to suppress the side-modes for the single mode operation.

Optics EXPRESS

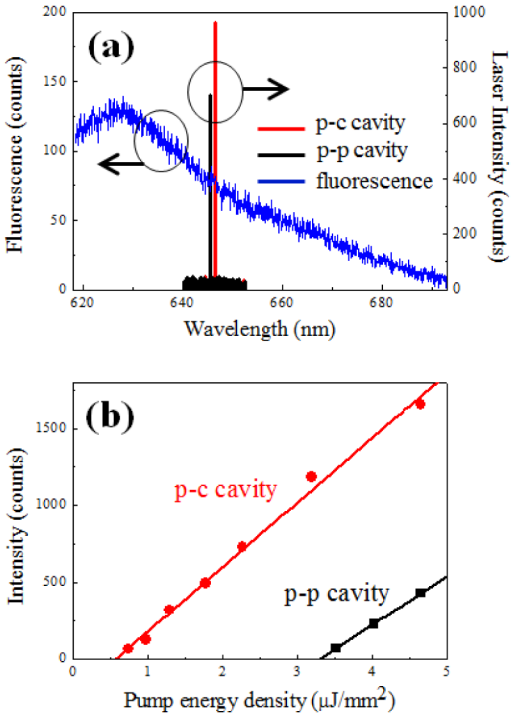

Fig. 2. Lasing characteristics of the LC laser. (a) Laser emission spectra: the p-c cavity laser is pumped with OPO at the pump energy density of 3.2 μJ/mm^2, while the p-p cavity laser is pumped at 11.1 μJ/mm^2. Note that the signal below lasing threshold shows fluorescence from the DCM dye as indicated by blue curve. Absolute value of the intensities cannot be compared, since different gratings of the spectrometer were used to obtain lasing and fluorescence spectra. (b) Spectrally integrated laser intensity as a function of the pump energy density. A linear fit of the laser intensities from the p-c cavity laser (red) results in a corresponding lasing threshold of approximately 0.58 μJ/mm^2, whereas the p-p cavity laser (black) has 3.3 μJ/mm^2.

The LC laser with p-c FP microcavity shows clear lasing characteristics with a lasing threshold as low as 0.58 μJ/mm^2, as presented in the red linearly fitted line of Fig. 2(b). Considering the size of the p-c cavity (microwell diameter is approximately 40 μm.), the lasing threshold in terms of total pump energy is approximately 0.73 nJ, whereas existing band-edge lasers exhibit lasing thresholds a few orders of magnitude higher [12, 17, 23, 24]. For comparison between the p-c and p-p cavities, spectrally integrated lasing intensities from a part of the LC-filled sandwich cell without the microwell are also measured. This FP microcavity thus has p-p structure with the same DBR mirrors, and is expected to have lower Q-factor than the p-c FP microcavity. Even though the p-p cavity laser also shows clear lasing characteristics, its lasing threshold is approximately 3.3 μJ/mm^2, over 5-fold increase as compared to the p-c cavity laser. The p-p cavity lasing spectrum at the pump energy density of 11.1 μJ/mm^2 is depicted by the black curve in Fig. 2(a), along with the fluorescence spectrum when the pump is below the lasing threshold. As investigated in the previous work [18], the higher lasing threshold of the p-p cavity laser is due to the lower Q-factor, which is caused by inevitable subtle misalignment during the assembly. The Q-factor of the p-c cavity and p-p cavity estimated from the lasing threshold and the lasing spectra are 8300 and 2900, respectively (corresponding finesses are 212 and 75, respectively). Even though the p-c cavity with a deeper microwell gives larger improvement in the finesse and the Q-factor, as explored in the previous work [16], shallower p-c cavity is chosen for reliable planar alignment of the nematic LC molecules without the applied voltage. Most importantly, the lower lasing threshold caused by the high Q-factor is a direct proof that our LC laser has superior lasing

Optics EXPRESS

characteristics compared to a conventional FP microcavity laser, as well as band-edge LC lasers. Furthermore, it is possible to produce an array of LC lasers with the p-c FP microcavities, when a larger area of the sandwich cell including multiple microwells is pumped simultaneously with the pump energy intensity set between the lasing thresholds of the p-c cavity laser and p-p cavity laser.

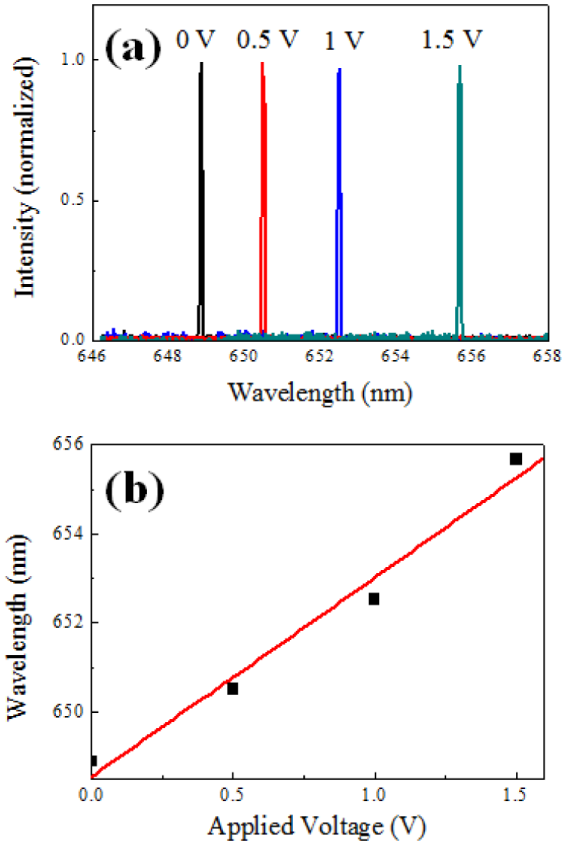

Fig. 3. Wavelength tuning of the LC laser by varying applied voltage. (a) When no voltage is applied to the sandwich cell, the laser shows single-mode emission at 648.9 nm. As the electric field increases, the laser emission wavelength continuously red-shifts. For example, when 1.5 V is applied, the wavelength produced is 655.7 nm, which is 6.8 nm longer than that of the 0 V case. (b) Linear fit of the wavelength tuning. The slope is 4.5 nm/V.

As described earlier, the light propagating inside the microcavity experiences the effective refractive index of 1.61, owing to the alignment of the LC molecules parallel to the glass substrate with random azimuthal angles. Meanwhile, when voltage is applied between the top and bottom ITO electrodes of the sandwich cell, the electric field inside the microcavity induces homeotropic alignment of the LC molecules, as illustrated in Fig. 1(b). When all the LC molecules are aligned parallel to the light propagating direction, their long axes are always perpendicular to the polarization of the light despite the azimuthal angles, and thus the light experiences the ordinary refractive index, n_o, of the LC medium. n_o of 5CB is 1.53 at 650 nm wavelength [22], which results in an effective index of the entire laser cavity decreased by 0.08, as well as longer wavelength laser emission. As depicted in Fig. 3, the laser wavelength continuously redshifts from 648.9 nm, as voltage is applied to the top and bottom electrodes. When 1.5 V is applied, the emission wavelength is shifted by 6.8 nm (emission wavelength = 655.7 nm), as compared to the laser without an applied voltage.

Optics EXPRESS

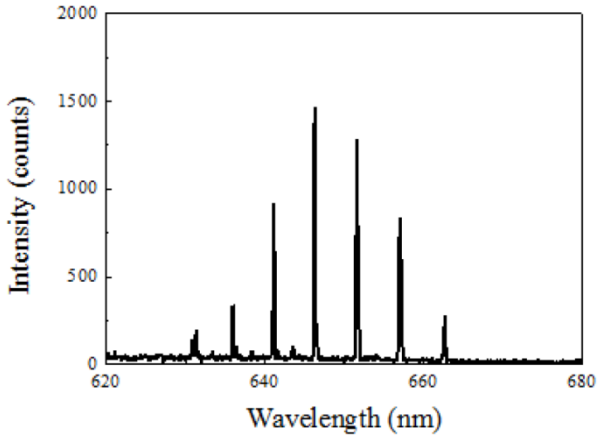

Fig. 4. Laser emission spectrum of the LC laser with a larger sandwich cell gap (20 μm), when pumped with the pump energy density of 3.2 μJ/mm^2. The signal shows a multi-mode laser emission with the FSR of 5.3 nm.

In theory, the FSR of the FP laser cavity is inversely proportional to the cell gap, and without path loss, the lasing threshold also decreases with increased FP cavity length. Figure 4 presents the lasing spectrum of the same LC laser with an increased sandwich cell gap of 20 μm. The spectrum shows multi-wavelength laser emission with the FSR of 5.3 nm, whereas the 5-μm-cell-gap LC laser has a clear single-wavelength emission. The estimated FSR matches well with calculations considering an increased cavity length (23 μm, combining the cell gap and the average microwell depth), thus the cell gap should be maintained no larger than 5 μm in order to guarantee the single-mode laser operation. The larger cell gap laser has a lasing threshold of 0.66 μJ/mm^2, which is similar to that of the smaller cell gap laser. This is due to the path loss, such as diffraction loss and medium absorption, thus there is no advantage in selecting the cell gap larger than 5 μm. From this demonstration, we can foresee that our LC laser is capable of a single wavelength lasing with any LC-dispersible dye, simply by limiting the sandwich cell gap for a sufficiently large FSR.

4. Summary

In summary, we have demonstrated a LC laser based on a p-c FP microcavity with a dye-doped nematic LC gain medium in the sandwich cell. The LC laser exhibits a lasing threshold several orders of magnitude lower than the existing band-edge LC laser and is capable of continuous tuning of emission wavelength by simply applying voltage. Because the laser is based on a common nematic LC material, it can be operated at room temperature and has stable performance in the wide temperature change. The proposed scheme resembles a simple VA-LCD device, thus can accommodate various commercial LCD technologies and has great potential as a tunable laser light source for μTAS.

Funding

National Research Foundation (NRF) Korean Government (MSIP) (2012M3A7B4049802); National Science Foundation (ECCS-1607250, DBI-1451127); National Institutes of Health (NIBIB-1R21EB016783); National Science Foundation of China (Grant No. 61471254).

68.203.167.239 {ts '2017-01-11 14:00:01'}